

Axion gegenschein

Radio counter-sources from axion decay

Oindrila Ghosh

September 10, 2019

(with Jordi Miralda-Escudé)

Institute of Cosmos Sciences, University of Barcelona (ICCUB)

Table of contents

1. Axion gegenschein
2. Background and sensitivity
3. Radio observation
4. Conclusions

Axion gegenschein

Axions: spontaneous and stimulated emission

Interaction term for axions and photons

$$\mathcal{L}_{a\gamma\gamma} = -\frac{1}{4}g_{a\gamma\gamma}aF_{\mu\nu}\tilde{F}_{\mu\nu} \quad (1)$$

with axion mass

$$m_a = 6 \times 10^{-6} \text{eV} \left(\frac{10^{12} \text{GeV}}{f_a} \right) \quad (2)$$

Axion decay $a \rightarrow \gamma\gamma$

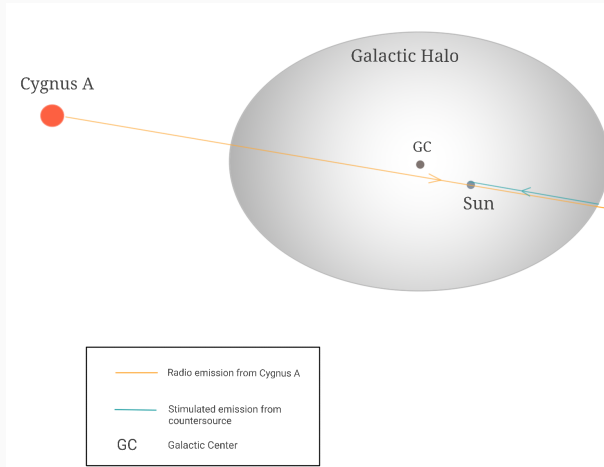
$$\tau_a = \frac{64\pi}{m_a^3 g_{a\gamma\gamma}^2} \quad (3)$$

Contribution of CMB, galactic, and extragalactic background

$$f_\gamma(\ell, \Omega, m_a) \simeq f_{\gamma, \text{CMB}}(m_a) + f_{\gamma, \text{gal}}(\ell, \Omega, m_a) + f_{\gamma, \text{ext-bkg}}(m_a) \quad (4)$$

Axion gegenschein

Stimulated emission → Backscattering of astrophysical radio pulses in the MW Halo

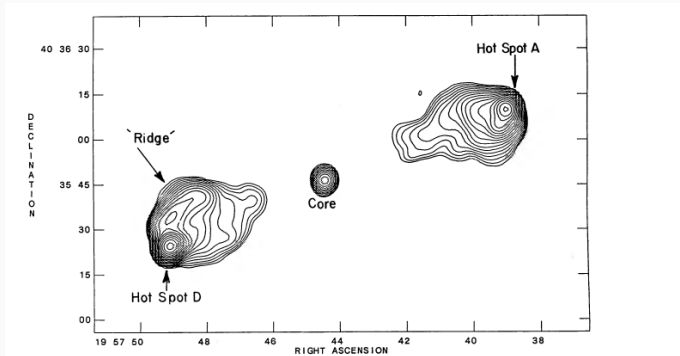


Axion gegenschein in the Milky Way's dark matter halo

Source selection

Flux density of Cygnus A

$$S_{\text{CygA}} = S_0 \left(\frac{\nu}{\nu_0} \right)^{-0.58} \quad (5)$$



Radio contours of Cygnus A

Projection of dark matter undergoing stimulated emission along line of sight \rightarrow Counterimage/countersource

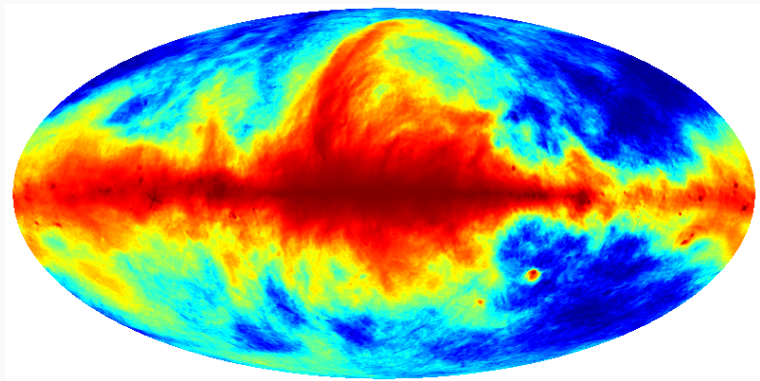
Characteristics:

- Size comparable to source size
- Aberration owing to velocity dispersion \perp l.o.s.

Background and sensitivity

Background and sensitivity

Galactic and extragalactic background in synchrotron radio emission



408-MHz Haslam all-sky map

Background and sensitivity

Radio power from the countersource:

$$P_{\text{radio}} = \frac{1}{16} g_{a\gamma\gamma}^2 \rho \left(\frac{dP_0}{d\nu} \right) \Big|_{\nu = \frac{m_a}{4\pi}} t \quad (6)$$

Spectral power of the astrophysical source (Cygnus A):

$$\frac{dP_0}{d\nu} = S_{\text{total}} A_{\text{eff}} \quad (7)$$

where

$$A_{\text{eff}} = \eta A_{\text{coll}} \quad (8)$$

Background and sensitivity

S_{total} : Total flux density evaluated at $\nu = m_a/4\pi$

SKA-low

Dipole array with number of elements $\sim 131,000$

Collection area (A_{coll}) $\sim 419,000 \text{ m}^2$

SKA-mid

$N_{tele} \sim 5600$

Diameter $D=15 \text{ m}$ for each dish

Efficiency of SKA: $\eta = 0.8$

Detectable radio power

$$P_{\text{radio}} = \left[\frac{dP_{\text{min}}}{d\nu} \Delta\nu \right] \Big|_{\nu = \frac{m_a}{4\pi}} \quad (9)$$

Minimum detectable spectral power

$$\frac{dP_{\text{min}}}{d\nu} = \frac{2T_{\text{sys}}}{\sqrt{t_{\text{obs}} \Delta B}} \quad (10)$$

$$\Delta B = \Delta\nu = \nu \sigma_{\text{disp}} \quad (11)$$

System noise temperature

$$T_{\text{sys}} = T_{\text{sky}} + T_{\text{rcvr}} \quad (12)$$

Atmospheric noise temperature

$$T_{\text{sky}} = 60 \left(\frac{\lambda}{1\text{m}} \right)^{2.55} = 60 \left(\frac{300\text{MHz}}{\nu} \right)^{2.55} \quad (13)$$

and

$$T_{\text{rcvr}} = 20\text{K (SKA-mid)}$$

$$T_{\text{rcvr}} = 40\text{K (SKA-low)}$$

$$\left[\frac{dP_{\min}}{d\nu} \Delta\nu \right] \Big|_{\nu=\frac{m_a}{4\pi}} = \frac{1}{16} g_{a\gamma\gamma}^2 S_{\text{Cygnus A}} \Big|_{\nu=\frac{m_a}{4\pi}} A_{\text{eff}} \int_0^\infty \rho(r) dx \quad (14)$$

Dark matter density in the MW Halo follows the NFW profile

$$\rho(r) = \frac{\delta_c \rho_c}{(r/r_s)(1+r/r_s)^2} \quad (15)$$

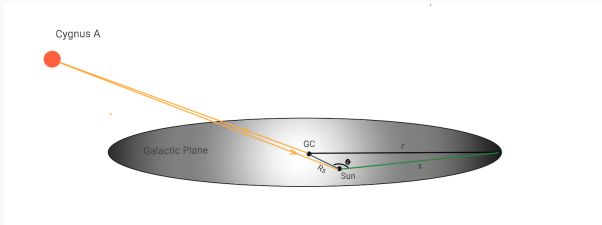
Background and sensitivity

Integration is performed numerically using

$$r^2 = x^2 + R_s^2 - 2xR_s \cos \theta \quad (16)$$

$R_s = 8$ kpc, distance of Sun from the Galactic Center

r : radial distance



A geometric construction to illustrate the integration variable

θ : Angular separation between Cygnus A and the Sun w.r.t. the Galactic Center

Radio observation

Single-dish observation

Angular resolution

$$\theta_{FWHM} \simeq 1.22 \frac{\lambda}{D} \simeq 0.7^\circ \left(\frac{1\text{GHz}}{\nu} \right) \left(\frac{15\text{m}}{D} \right) \quad (17)$$

Noise temperature of the instrument

$$T_{\text{ant}} = \frac{A_{\text{eff}} \langle S \rangle}{2k_b} \quad (18)$$

For each telescope

$$\left(\frac{S}{N} \right)_{sd, \text{single}} = \frac{T_{\text{ant}}^{\text{pb}}}{T_{\text{min}}} \quad (19)$$

For an array of single-dish telescopes

$$\left(\frac{S}{N} \right)_{sd, \text{array}} = \sqrt{N_{\text{tele}} n_{\text{pol}}} \left(\frac{S}{N} \right)_{\text{single}} = \sqrt{N_{\text{tele}} n_{\text{pole}}} \frac{T_{\text{ant}}^{\text{pb}}}{T_{\text{min}}} \quad (20)$$

Observation in the interferometric mode

Angular resolution of primary beam

$$\theta_{pb} = 12.5' \left(\frac{1\text{GHz}}{\nu} \right) \left(\frac{100\text{m}}{D} \right) \quad (21)$$

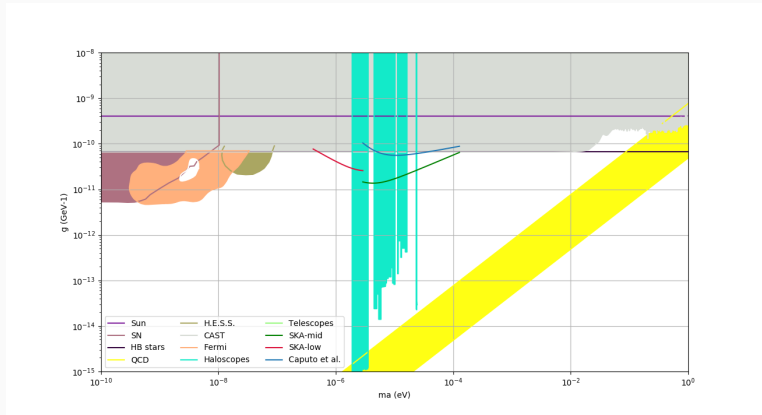
Minimum detectable flux density

$$S_{\min} = \text{SNR} \frac{\text{SEFD}}{\sqrt{n_{\text{pol}} \Delta B t_{\text{obs}}}} \quad (22)$$

with

$$\text{SEFD} = \frac{T_{\text{sys}}(\nu)}{G} \quad (23)$$

Phenomenological implications



Axion mass vs. axion photon coupling. Limits shown are for axion gegenchein using SKA-mid (green) and SKA-low (red) sensitivities. Bounds from stimulated emission in dSphs shown in blue [Caputo et al. (2018)]

Conclusions

Key takeaways and further explorations

- Astrophysical radio pulses from galactic and extragalactic sources can induce stimulated emission in the Milky Way's halo.
- Stimulated emission from halo dark matter can lead to a detectable signal at future-generation radio telescopes with conservative SNR ~ 1 .
- *Axion gegenschein* provides **100-fold increase in radio sensitivity compared to contemporary frameworks!**
- Detection of fainter countersources feasible with improved radio sensitivity in the future.
- Axion gegenschein opens up a new indirect detection scheme for dark matter. Several other radio-loud sources could provide optimal stimulated emission.
- Further boost in (stimulated) radio emission can occur owing to dwarfs along the line of sight.

Thank you for your attention!

Questions?

In terms of the electric and magnetic fields, $\vec{E}(x)$ and $\vec{B}(x)$:

$$\mathcal{L}_{a\gamma\gamma} = -g_{a\gamma\gamma} \frac{\alpha}{\pi} \frac{1}{f_a} a(x) \vec{E}(x) \cdot \vec{B}(x), \quad (24)$$

Strong CP problem and Peccei-Quinn symmetry breaking

CP-violating term leading to neutron EDM

$$\mathcal{L}_{\theta, \text{QCD}} = \frac{\theta_{\text{QCD}}}{32\pi^2} \text{Tr} G_{\mu\nu} G^{\mu\nu} \quad (25)$$

→ Axions as pseudo-Goldstone bosons arising from spontaneous breaking of PQ symmetry

→ Dynamical non-perturbative solution of the CP problem using dilute instanton gas approximation

$$m_{a, \text{QCD}} \approx 6 \times 10^{-6} \text{eV} \left(\frac{10^{12} \text{GeV}}{f_{a/C}} \right) \quad (26)$$

Several theoretical frameworks including Peccei-Quinn-Wilczek-Weinberg (PQWW), Kim-Shifman-Vainshtein-Zakharov (KSVZ), & Dine-Fischler-Srednicki-Zhitnitsky (DFSZ) formalisms.

Observation in the interferometric mode

For each synthesized beam in the interferometric mode, angular resolution

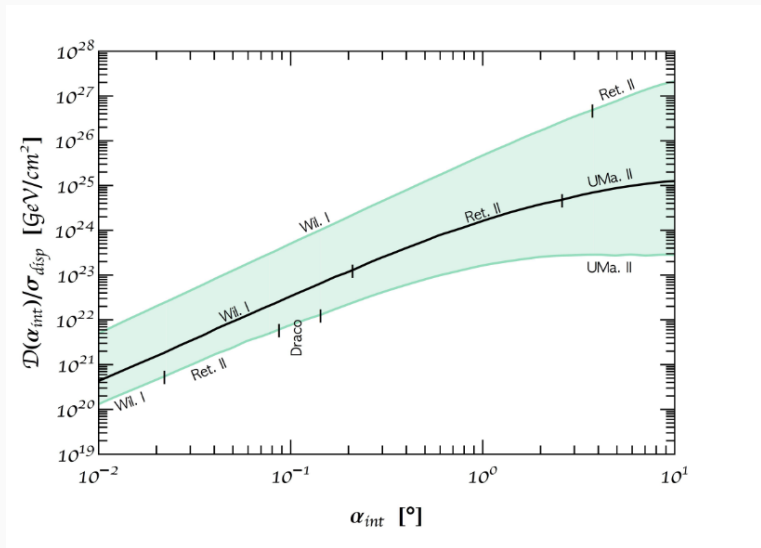
$$\theta_{\text{synth}} \approx 50'' \left(\frac{1\text{GHz}}{f} \right) \left(\frac{1\text{km}}{B_{\text{max}}} \right) \quad (27)$$

SNR is expressed as $\sqrt{\delta\chi^2}$

$$\delta\chi^2 = n_{\text{pol}} t_{\text{obs}} G_{\text{array}}^2 \sum_{i=1}^{N_{\text{synth}}} \frac{F_i^2}{B_i T_i^2} \quad (28)$$

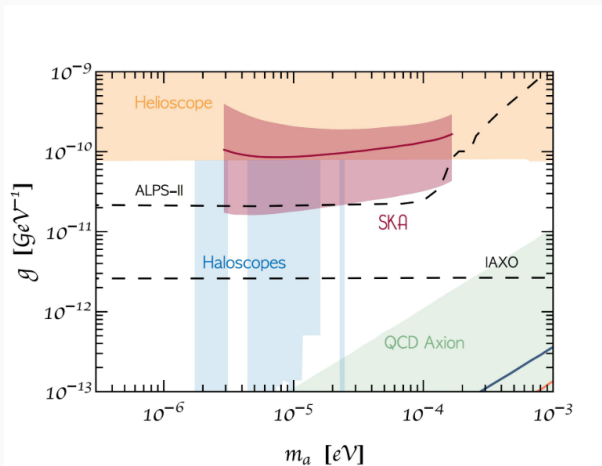
Scaling relation for antenna gain $G_{\text{array}} \sim N_{\text{tele}} (N_{\text{tele}} - 1) G$

Radio signal from dwarfs



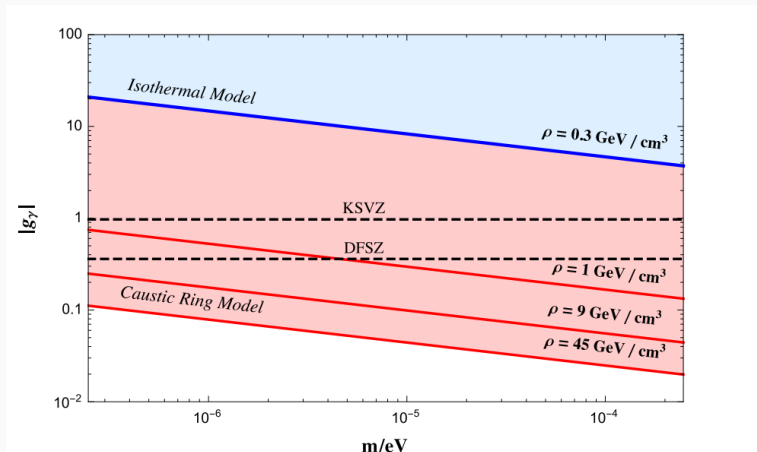
$D(\alpha_{int})/\sigma_{disp}$ as a function of the field of view of the telescope

Radio signal from dwarfs









Sensitivity of SKA in the $g_{a\gamma\gamma} - m_a$ parameter space denoted using median $\pm 95\%$ confidence interval in the dSph with largest


Radio signal from echo wave



Sensitivity in $|g_\gamma|$ vs. axion mass m_a for an outgoing power of 10 MW/year [Sikivie et al. (2019)]

-  Borka Jovanovic, V., & Urosevic, D. (2011). Temperature, brightness and spectral index of the Cygnus radio loop. *Mexican magazine of astronomy and astrophysics* , 47 (1), 159-171.
-  Carilli, C. L., Perley, R. A., Dreher, J. W., & Leahy, J. P. (1991). Multifrequency radio observations of Cygnus A-Spectral aging in powerful radio galaxies. *The Astrophysical Journal*, 383, 554-573.
-  SKA Science Imaging Performance. <https://www.skatelescope.org/wp-content/uploads/2014/03/SKA-TEL-SCI-SKO-SRQ-001-1-Level-0-Requirements-1.pdf>

-  SKA Whitepaper, Retrieved May 26, 2019, from <https://www.skatelescope.org/wp-content/uploads/2014/03/SKA-TEL-SKO-0000308-SKA1-System-Baseline-v2-Descriptor.pdf>
-  Haslam, C. G. T., Klein, U., Salter, C. J., Stoffel, H., Wilson, W. E., Cleary, M. N., ... & Thomasson, P. (1981). A 408 MHz all-sky continuum survey. I-Observations at southern declinations and for the North Polar region. *Astronomy and Astrophysics*, 100, 209-219.
-  Caputo, A., Garay, C. P., & Witte, S. J. (2018). Looking for axion dark matter in dwarf spheroidal galaxies. *Physical Review D*, 98(8), 083024.

-  Arza, A. (2019). Photon enhancement in a homogeneous axion dark matter background. *The European Physical Journal C*, 79(3), 250.
-  Caputo, A., Regis, M., Taoso, M., & Witte, S. J. (2019). Detecting the stimulated decay of axions at radio frequencies. *Journal of Cosmology and Astroparticle Physics*, 2019(03), 027.